Biogeochemistry and biodiversity of methane cycling in subsurface marine sediments (Skagerrak, Denmark)

Article *in* Environmental Microbiology · June 2007

Impact Factor: 6.2 · DOI: 10.1111/j.1462-2920.2006.01237.x · Source: PubMed

13 authors, including:

Ronald John Parkes
Cardiff University
151 PUBLICATIONS **7,590** CITATIONS
SEE PROFILE

Fiona Brock
Cranfield University
86 PUBLICATIONS **1,747** CITATIONS
SEE PROFILE

Gordon Webster
Cardiff University
65 PUBLICATIONS **2,796** CITATIONS
SEE PROFILE

Joachim Rinna
Det Norske Oljeselskap ASA
16 PUBLICATIONS **501** CITATIONS
SEE PROFILE

Environmental Microbiology (2007) **9**(5), 1146–1161 doi:10.1111/j.1462-2920.2006.01237.x

Biogeochemistry and biodiversity of methane cycling in subsurface marine sediments (Skagerrak, Denmark)

R. John Parkes,[1]* Barry A. Cragg,[1] Natasha Banning,[2†] Fiona Brock,[1‡] Gordon Webster,[1,2] John C. Fry,[2] Ed Hornibrook,[3] Richard D. Pancost,[4] Sam Kelly,[4] Nina Knab,[5] Bo B. Jørgensen,[5] Joachim Rinna[1] and Andrew J. Weightman[2]

[1]*School of Earth, Ocean and Planetary Sciences, Cardiff University, Main Building, Park Place, Cardiff CF10 3YE, UK.*

[2]*Cardiff School of Biosciences, Cardiff University, Main Building, Park Place, Cardiff CF10 3TL, UK.*

[3]*Bristol Biogeochemistry Research Centre, Department of Earth Sciences, University of Bristol, Wills Memorial Building, Queens Road, Bristol BS8 1RJ, UK.*

[4]*School of Chemistry, University of Bristol, Cantocks Close, Bristol BS8 1TS, UK.*

[5]*MPI for Marine Microbiology, Celciusstr. 1, 28359 Bremen, Germany.*

Summary

This biogeochemical, molecular genetic and lipid biomarker study of sediments (~4 m cores) from the Skagerrak (Denmark) investigated methane cycling in a sediment with a clear sulfate-methane-transition zone (SMTZ) and where CH_4 supply was by diffusion, rather than by advection, as in more commonly studied seep sites. Sulfate reduction removed sulfate by 0.7 m and CH_4 accumulated below. ^{14}C-radiotracer measurements demonstrated active H_2/CO_2 and acetate methanogenesis and anaerobic oxidation of CH_4 (AOM). Maximum AOM rates occurred near the SMTZ (~3 nmol cm^{-3} day^{-1} at 0.75 m) but also continued deeper, overall, at much lower rates. Maximum rates of H_2/CO_2 and acetate methanogenesis occurred below the SMTZ but H_2/CO_2 methanogenesis rates were × 10 those of acetate methanogenesis, and this was consistent with initial values of ^{13}C-depleted CH_4 ($\delta^{13}C$ *c.*–80‰). Areal AOM and methanogenic rates were similar (~1.7 mmol m^{-2} day^{-1}), hence, CH_4 flux is finely balanced. A 16S rRNA gene library from 1.39 m combined with methanogen (T-RFLP), bacterial (16S rRNA DGGE) and lipid biomarker depth profiles showed the presence of populations similar to some seep sites: ANME-2a (dominant), ANME-3, *Methanomicrobiales*, *Methanosaeta Archaea*, with abundance changes with depth corresponding to changes in activities and sulfate-reducing bacteria (SRB). Below the SMTZ to ~1.7 m CH_4 became progressively more ^{13}C depleted ($\delta^{13}C$ –82‰) indicating a zone of CH_4 recycling which was consistent with the presence of ^{13}C-depleted archaeol ($\delta^{13}C$ –55‰). Pore water acetate concentrations decreased in this zone (to ~5 μM), suggesting that H_2, not acetate, was an important CH_4 cycling intermediate. The potential biomarkers for AOM-associated SRB, non-isoprenoidal ether lipids, increased below the SMTZ but this distribution reflected 16S rRNA gene sequences for JS1 and OP8 bacteria rather than those of SRB. At this site peak rates of methane production and consumption are spatially separated and seem to be conducted by different archaeal groups. Also AOM is predominantly coupled to sulfate reduction, unlike recent reports from some seep and gassy sediment sites.

Introduction

Global methane production in marine sediments is very significant at between 75 and 320 Tg $year^{-1}$ (Valentine, 2002) and these sediments also contain the largest global reservoir of methane (Kvenvolden, 1988). However, nearly all the methane moving upwards to the sediment surface is microbially oxidized, with anaerobic oxidation coupled to sulfate reduction playing the major role (80%; Orphan *et al.*, 2001). Most of our knowledge about the microbiology and controls on anaerobic oxidation of methane (AOM) have come from studies and experiments on seep and gas hydrate sediments (e.g. Hinrichs *et al.*, 1999; Boetius *et al.*, 2000; Knittel *et al.*, 2005; Niemann *et al.*, 2005; Treude *et al.*, 2005a; Fang *et al.*, 2006). These studies demonstrate that a unique group of *Archaea*, ANME, mainly within the methanogenic *Methanosarcinales*, are responsible for AOM usually in association with sulfate-reducing bacteria (SRB), which are often members of the *Desulfosarcina–Desulfococcus* group

Received 15 December, 2006; accepted 18 December, 2006.
*For correspondence. E-mail J.Parkes@earth.cf.ac.uk; Tel. (+44) 29 2087 0058; Fax (+44) 29 2087 4326. Present addresses: †School of Earth and Geographical Sciences, University of Western Australia, Stirling Hwy, Crawley 6009, Australia; ‡Oxford Radiocarbon Accelerator Unit, Research Laboratory for Archaeology and History of Art, Dyson Perrins Building, South Parks Road, Oxford OX1 3QY, UK.

(DSS, Orphan *et al*., 2001; Knittel *et al*., 2005). Different groups of ANME (1a, 1b, 2a, 2b, 2c, 3) have now been detected which seem to dominate AOM in various locations, e.g. ANME-2a in Hydrate Ridge *Beggiatoa* mat, ANME-2c in Hydrate Ridge *Calyptogena* field, ANME-1 in a Black Sea microbial mat (Knittel *et al*., 2005) and ANME-1b North Sea gas seep (Niemann *et al*., 2005).

There are, however, much larger areas of non-seep marine sediments which have a discreet sulfate-methane-transition-zone (SMTZ) associated with AOM (e.g. Iversen and Jørgensen, 1985) and diffusion of *in situ* produced methane from below, but these have been much less studied. One non-seep study of shallow water, gassy sediments from the German Baltic Sea (Eckernforde Bay, Treude *et al*., 2005b) demonstrated that AOM was probably conducted by ANME-2 *Archaea*, and hence, was similar to some seep sites, but that it was not directly coupled to sulfate reduction, which is different from the majority of seep sites. It is therefore important to conduct further research into the process of AOM in other non-seep marine sediments to confirm whether these findings are generally applicable. In addition, as methane production and AOM occur in close proximity to each other at sites controlled by diffusion, their study may help to clarify whether these processes are being conducted by separate groups of *Archaea* or by one group with the ability to catalyse methane production or consumption depending upon prevailing environmental conditions, as has been recently suggested (Orcutt *et al*., 2005). In addition, there is little direct information about the relative distribution of AOM and methanogenic populations in marine sediments. We conducted an integrated biogeochemical, molecular genetic and lipid biomarker investigation of diffusively controlled sediments in the Danish Skagerrak to address these issues, as this site has sulfate, methane and AOM depth profiles (Iversen and Jørgensen, 1985) typical of large areas of marine sediments. In addition, biomarker evidence for AOM had been previously detected in a geographically close location in the Kattegat, the strait between Denmark and Sweden (Bian *et al*., 2001).

Results

Prokaryotic activity

Sulfate reduction was concentrated in the top 0.7 m as sulfate concentrations decreased from 25 mM to < 1 mM over this interval (Fig. 1A). When sulfate had reached these low concentrations methane increased rapidly to about 1.3 mM and remained high in deeper layers of the ~4 m core. This reflects the ability of SRB to outcompete methanogens for common substrates, and hence, most sulfate has to be removed before significant methane is produced (Lovley and Chapelle, 1995). Therefore, there was a very sharp SMTZ between ~0.6 and 0.8 m. Within this zone AOM rates were at a maximum (Fig. 1B; $P = 0.004$), reaching ~3.3 nmol cm^{-3} day^{-1}. However, in deeper layers AOM was still measurable and on average about five times higher (0.40 nmol cm^{-3} day^{-1}) than rates above the SMTZ. In addition, there was a single elevated AOM value at ~1.5 m ($P = 0.018$). Methanogenesis using H_2/CO_2 was the dominant methane formation pathway throughout the sediment (~10× acetate methanogenesis, Fig. 1C and D) albeit at peak rates approximately five times lower than for AOM. Although rates of H_2/CO_2 methanogenesis began to increase with depth below about 0.2 m, within the sulfate reduction zone, there was a broad stimulation in rates just below the SMTZ (0.87–1.34 m, max 416 pmol cm^{-3} day^{-1}). In deeper layers H_2/CO_2 methanogenesis continued to increase stepwise reaching maximum rates of 690 pmol cm^{-3} day^{-1} at ~3 m ($P < 0.001$). Low rates of acetate methanogenesis also occurred in the near surface sulfate reduction zone, although acetate oxidation in this zone was much higher (maximum rates of acetate oxidation and acetate methanogenesis were 14 nmol cm^{-3} day^{-1} and 20.8 pmol cm^{-3} day^{-1} at 0.6 m respectively). Acetate oxidation rates, however, decreased markedly below the sulfate reduction zone (average 0.6 nmol cm^{-3} day^{-1}; $P = 0.002$) while rates of acetate methanogenesis increased to a maximum (167 pmol cm^{-3} day^{-1} at ~2 m; $P < 0.01$). Interestingly, acetate methanogenesis rates in the zone of intense AOM were 0 or very close to 0. Measured rates of prokaryotic activity were in agreement with the wide range of rates recently measured in seeps and non-seep sediments (AOM 0.5–160 nmol cm^{-3} day^{-1}, H_2/CO_2 methanogenesis < 0.4–30 nmol cm^{-3} day^{-1}, acetate methanogenesis 0.02–6 nmol cm^{-3} day^{-1}, Banning *et al*., 2005; Niemann *et al*., 2005; Orcutt *et al*., 2005; Treude *et al*., 2005b). Pore water acetate concentrations were generally low (mean ~10 μM, Fig. 1E) and overall increased with depth, although between 0.6 and 1.4 m there was a small decrease in acetate concentration (11.3–5 μM). Maximum acetate concentrations at 1.95 m (17 μM) corresponded with a small peak in acetate metabolism (Fig. 1D). Consistent with H_2/CO_2 methanogenesis being the dominant methane formation pathway and increasing with depth, methane was strongly ^{13}C depleted (Fig. 1F). Methane $\delta^{13}C$ values were initially *c.* −80‰ which is characteristic for H_2/CO_2 methanogenesis (Whiticar, 1999), and then progressively became more ^{13}C-enriched with depth ($r = 0.93$ $P << 0.002$) as more and more of the $^{12}CO_2$ pool was used, forcing increasing amounts of residual $^{13}CO_2$ to be used for CH_4 formation ($\delta^{13}C$-CH_4 −73‰ at 4.1 m). A clear deviation from this trend occurred between about 0.7 and 1.7 m where $\delta^{13}C$-

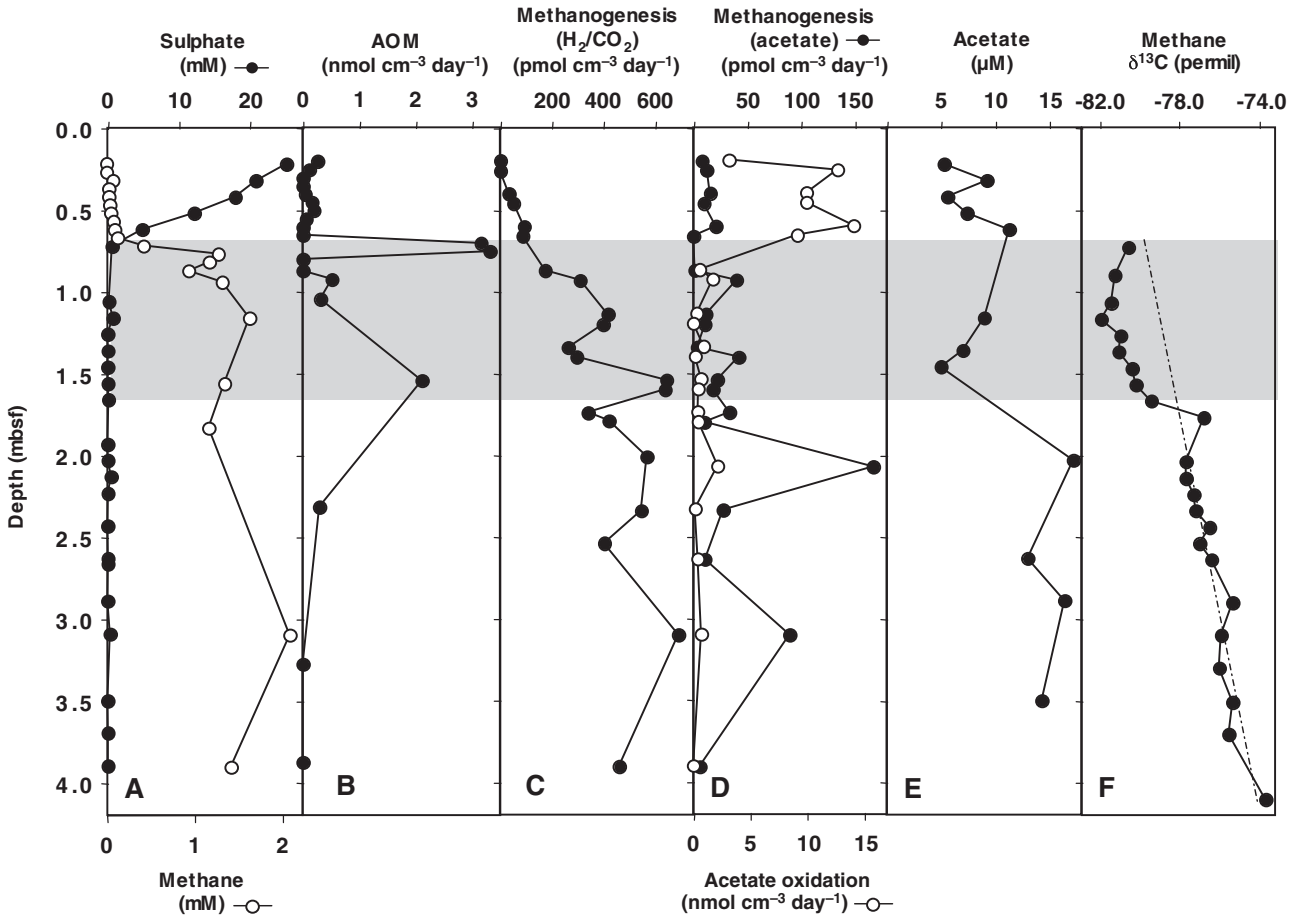

Fig. 1. Biogeochemical and prokaryotic activity depth profiles of Skagerrak sediments. Shaded box denotes zone of CH_4 recycling defined by the zone of deviation from the depth trend of increasing $\delta^{13}C$ of CH_4, shown as a dotted line in graph F.

CH_4 values become more depleted, reaching the most negative value of approximately –82‰.

Prokaryotic biomass and diversity

Total prokaryotic cell numbers (Fig. 2A) and percentage of dividing and divided cells (Fig. 2B) were high in the near surface (3.27×10^9 cm^{-3} and 14.7% respectively) and overall decreased with depth. However, between 0.5 and 1.4 m the rate of decline in total cells decreased and by 0.7 m there was a significant ($P = 0.05$) increase in the numbers of divided and dividing cells. Between 1.4 m and ~2 m both total cell numbers and percentage of dividing and divided cells fluctuated. Below this total counts and percentage of dividing and divided cells gradually decreased reaching a minimum of 8.33×10^7 cm^{-3} and 4.5% respectively, with the exception of an increase in the percentage of dividing and divided cells in the deepest sample (12% at ~4 m).

A 16S rRNA gene clone library was constructed using specific methanogen primers (Banning *et al.*, 2005) from within the methanogenic zone (1.39 m, Fig. 1), as an important aspect of this investigation was to determine methanogen diversity in a diffusively controlled sediment. A strong polymerase chain reaction (PCR) product was obtained with primers for *Methanosarcinales* and *Methanomicrobiales* whereas those primers specific for *Methanobacteriales* and the *Methancoccales* gave no product. The resulting clone library (Fig. 3) was dominated by sequences related to the ANME-2a (55%) and ANME-3 (10%) groups (Knittel *et al.*, 2005) followed by *Methanomicrobiales* (17.5%), *Methanosaeta* (12.5%) and a deep branching group most closely associated with the *Methanosarcinales* (5%, Sk6C-18 and Sk6C-1). Similar 16S rRNA gene sequences were present in libraries using archaeal primers and methanogens were probably a significant proportion of the archaeal community as they were 20% of all sequences (N. Banning, J. Fry, A. Weightman and J. Parkes, unpublished results). The phylogenetic tree of the methanogen 16S rRNA gene library (Fig. 3) showed limited diversity and a majority of sequences most closely related to environmental clones

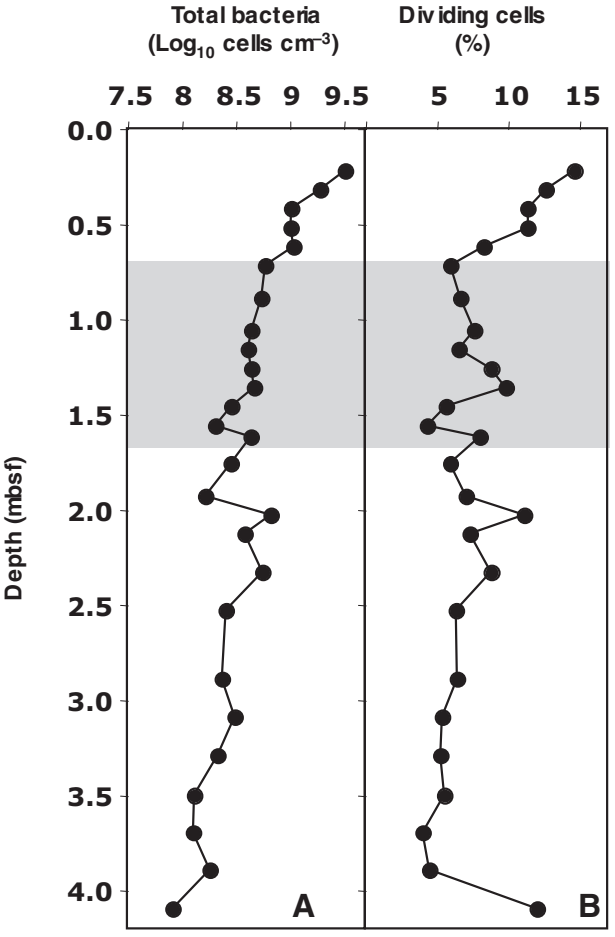

Fig. 2. Depth profile of (A) total prokaryotic cells and (B) percentage of dividing/divided cells in Skagerrak sediments. Shaded box denotes zone of CH_4 recycling defined by the zone of deviation from the depth trend of increasing $\delta^{13}C$ of CH_4 in Fig. 1F.

rather than cultured isolates (highest similarity to pure culture, 96%).

Prokaryotic biodiversity depth distributions

Methanogen sequences determined by terminal restriction fragment length polymorphisms (T-RFLP) with the same methanogen-specific 16S rRNA gene primers as used for the library were very similar to those identified by cloning and sequencing (Fig. 4). We have previously shown that T-RFLP analysis of defined methanogen mixtures accurately reflected the proportions of the different methanogens present (Banning *et al*., 2005), and hence, T-RF peak size measured here should also be a reliable measure of the proportions of methanogens present. Fragments were dominated by peaks assigned to *Methanomicrobiales* (139 bp), *Methanosarcinales*/ANME (277 bp) and *Methanosaeta* related (42 bp); at 33%, 29% and 19% respectively, mean for all depths. In addition, there were clear changes in populations with depth (Fig. 4): (i) *Methanomicrobiales* accounted for 22% of all fragments at 0.25 m and then increased with depth (to 55%), except for a minimum value at ~1 m (8%), (ii) *Methanosarcinales*/ANME fragments were at a maximum at 1 m (~73%) and then decreased with increasing depth. Below ~2 m the proportion of these fragments were relatively constant at ~20%, (iii) *Methanosaeta*-related fragments were low in the top metre (5%) and increased below (mean 25%) reaching a maximum at 1.86 m (40%). Three peaks detected by T-RFLP profiling could not be assigned to specific phylotypes; however, these only accounted for a mean of 2.6% of all fragments, maximum 36% (T-RF peak of 122 bp at 0.25 m, this overall decreased with depth).

T-RFLP and methanogen library results were in agreement which suggests that the molecular genetic data were robust. At 1.39 m the T-RF peak distribution and proportion of assigned clones in the library, respectively, were for ANME/*Methanosarcinales* 42% and 65%; for *Methanomicrobiales* 35% and 17.5% and for *Methanosaeta* related 16% and 12.5%. Although T-RF peak 42 could correspond to some but not all *Methanoculleus* species, as well as *Methanosaeta*, no *Methanoculleus* sequences were present in the clone library, although five *Methanosaeta* sequences were present (Fig. 3). Therefore, it seems likely that the 42 bp peak in these samples was predominantly from the acetate utilizing *Methanosaeta* group, and this is reinforced by the close relationship between the depth distribution of this peak and rates of acetate methanogenesis (Fig. 4D).

Bacterial depth profile data were obtained from 16S rRNA gene PCR-DGGE and band sequencing (Table 1). Fourteen phylotypes were detected, 13 of them different, and with the majority (90–100%) related to environmental clones from sediments or subseafloor sediments (Peru Margin, Sea of Okhotsk and Nankai Trough). These included sequences related to *Gammaproteobacteria*, *Deltaproteobacteria*, *Chloroflexi*, *Spirochaetes* and candidate divisions JS1 and OP8. Sequences loosely related (93%) to an uncultured *Deltaproteobacteria* DSS63 SRB sequence (*Desulfosarcina–Desulfococcus* group from marine Arctic sediments, Ravenschlag *et al*., 2000), which are part of AOM consortia in other environments (Knittel *et al*., 2005; Orcutt *et al*., 2005), were also present but only below the top 1 m. The only sequences closely related to cultured prokaryotes were the alphaproteobacterial sequences closely related to *Mesorhizobium* sp. RI01 (99%, from soybean rhizosphere, Peterson *et al*., 2006) which had distributions broadly similar to the *Methanomicrobiales*-related T-RF peaks (Fig. 4). Rhizobia recently have been shown to be widespread in subsurface marine sediments and some Rhizobia enrichments can grow anaerobically by fermentation and/or in syntrophic relationship (Süß *et al*., 2004). Bacterial DGGE

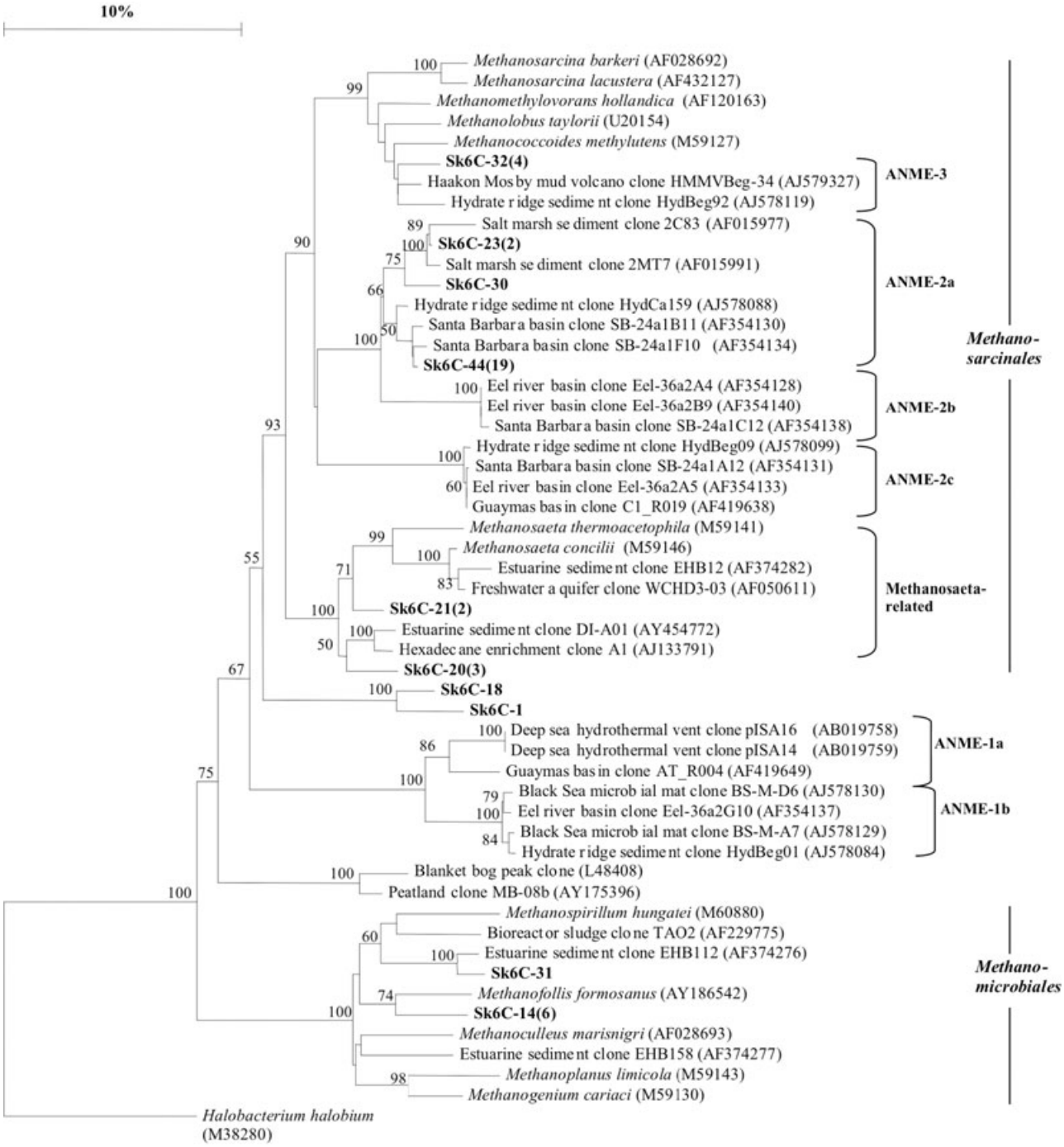

Fig. 3. Phylogenetic tree showing representative 16S rRNA gene sequences ($n = 40$) of methanogens from Skagerrak sediment at 1.39 m obtained by PCR cloning with primers 355F/1068R targeting the *Methanosarcinales* and *Methanomicrobiales*. Phylotypes exhibiting ≥ 97% sequence similarity are represented by one sequence with the total number of clones given in parenthesis. The tree was constructed by the neighbour-joining method using 561 aligned nucleotides with *Halobacterium halobium* as the outgroup. The scale bar represents 10% sequence similarity and bootstrap values were derived from 100 analyses (values < 50% are not shown). Library coverage was estimated to be 90%.

profiles demonstrated some broad agreement between the two different primers used (general bacterial and JS1 targeted) with *Gamma* and *Deltaproteobacteria* and JS1 sequences detected in both. These groups along with *Chloroflexi* and OP8 have commonly been detected in subsurface marine sediments (e.g. Reed *et al*., 2002; Inagaki *et al*., 2003; 2006; Parkes *et al*., 2005; Webster *et al*., 2006a).

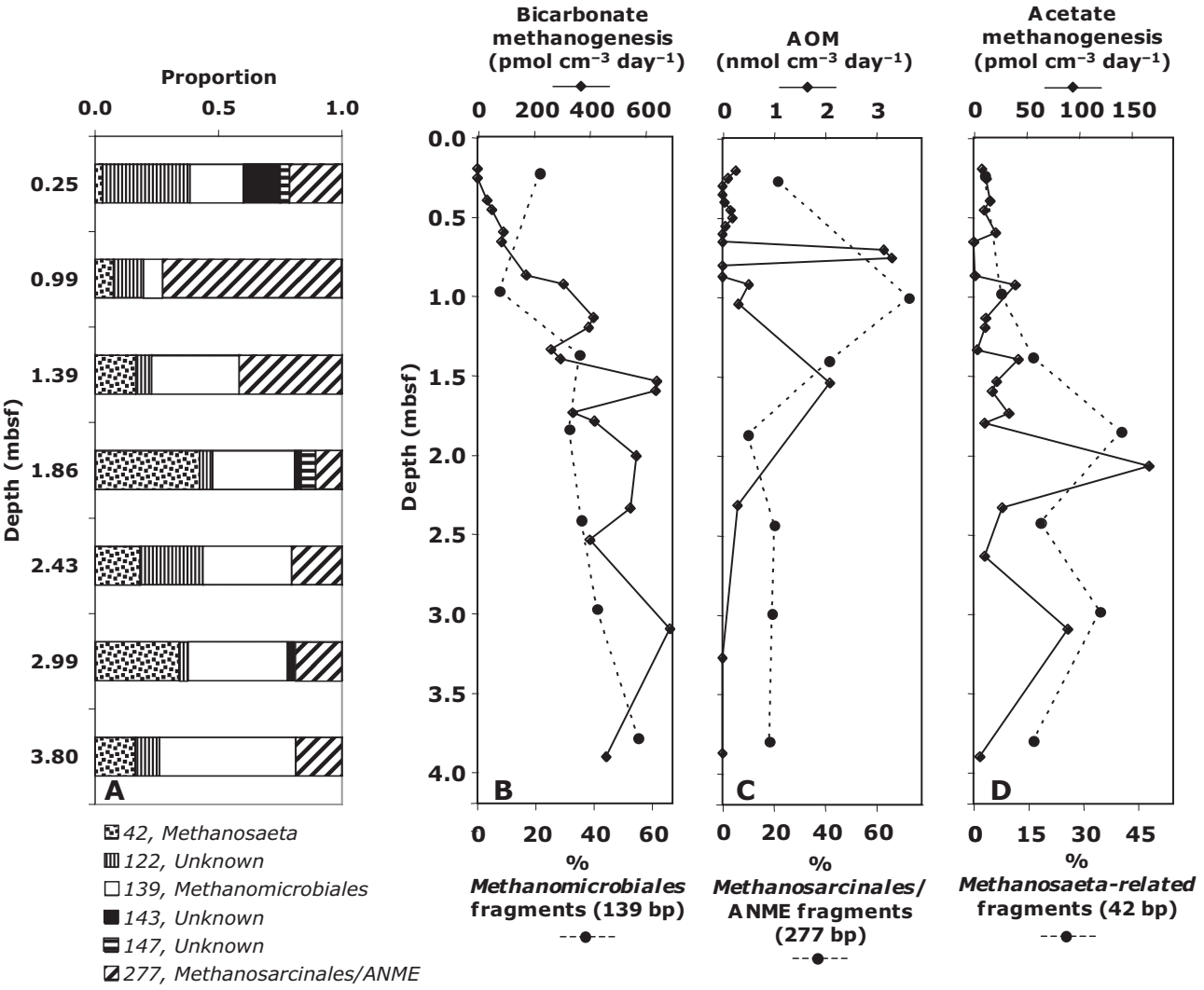

Fig. 4. Depth distributions of methanogen-related *Archaea* in Skagerrak sediments by T-RFLP analysis (A), depth relationships between percentage of *Methanomicrobiales* (B), *Methanosarcinales*/ANME (C) and *Methanosaeta*-related (D) T-RFs (see Table 2) and their potential activities.

Lipids were dominated by a variety of compounds, including n-alkanols with an even-over-odd predominance derived from terrestrial higher plants (Eglinton and Hamilton, 1967) and alkenones derived from haptophyte algae (Marlowe *et al*., 1984); thus, the overall organic matter assemblage reflects a mixed source from both terrestrial and 'labile' marine sources, as previously described (van Dongen *et al*., 2000). Bacterial and archaeal biomarkers were also present, albeit at much lower concentrations, and their distribution changed with depth (Fig. 5). The archaeal biomarkers present include archaeol (detected in both the phospholipids and neutral polar fractions), hydroxyarchaeol and PMI (2,6,10,15,19-pentamethylicosane). Due to sample size limitations phospholipids were only analysed in the Site 820 sister core. In that core, archaeol was detected after saponification; saponification is not a standard technique for cleaving polar head groups and so we do not interpret these data quantitatively, but the presence of archaeol in that fraction is strong evidence for an active population at the time of sampling. All three archaeal lipids occur in a range of *Archaea*, including methanogens, but the co-occurrence of all three compounds is typical for many AOM settings (e.g. Hinrichs *et al*., 2000; Pancost *et al*., 2001; Pancost and Damste, 2003; Zhang *et al*., 2003; Pancost *et al*., 2005; Bouloubassi *et al*., 2006). Archaeol abundances continually increase from 0.55 to 1.37 m, which is consistent with increasing rates of H_2/CO_2 methanogenesis and, below ~0.6 m, increasing CH_4 concentrations. Only one archaeol $\delta^{13}C$ value could be obtained, and this was from the phospholipid fraction at 1.02–1.12 m. Its $\delta^{13}C$ of –55‰, although not as depleted

Table 1. Identities of dominant DGGE bands detected by different nested PCR-DGGE methods in Skagerrak sediments (Heincke 191, 821 GC).

PCR-DGGE method	Phylogenetic group	Closest phylotype	Sequence similarity (%)	Distribution with depth (m)						
				0.25	0.99	1.39	1.86	2.43	2.99	3.80
16S rRNA gene general bacterial primers	*Gammaproteobacteria*	Bacterial clone JH12_C28 (Intertidal flat of Ganghwa island, unpublished)	92	+	•	•	•	•	•	•[a]
	Alphaproteobacteria	*Mesorhizobium* sp. RI01 (soybean rhizosphere, Peterson *et al*., 2006)	99	–	–	•	•	+	•	•
	Deltaproteobacteria	Bacterial clone: ODP1230B18.24 (Peru margin site 1230, Inagaki *et al*., 2006)	90	•	–	•	•	–	+	–
	Chloroflexi	Bacterial clone QLS40-B34 (Saline Qinghai Lake sediments, Dong *et al*., 2006)	99	•	•	•	+	–	+	–
	Spirochaetes	Spirochete clone IE053 (microbial mats of Ebro and Camargue Deltas, unpublished)	92–93	–	–	+	+	+	•	•
	JS1	Bacterial clone: OHKB2.83 (Deep sediment, Sea of Okhotsk, Inagaki *et al*., 2003)	91–95	–	•	•	•	+	+	•
16S rRNA gene JS1 primers	JS1	Uncultured bacterium clone: OHKB2.83 (Deep sediment, Sea of Okhotsk, Inagaki *et al*., 2003)	93–100	–	•	•	+	+	+	+
	JS1	Uncultured candidate division JS1 bacterium clone NANK-B7 (Nankai Trough, Newberry *et al*., 2004)	99	–	–	•	–	+	•	–
	JS1	Bacterial clone MA-A2-104 (Nankai Forearc Basin, Reed *et al*., 2002)	100	–	–	•	–	+	•	–
	OP8	Bacterial clone C1_B017 (Teske *et al*., 2002)	90–94	–	+	•	+	•	•	+
	OP8	Candidate division OP8 bacterial clone R76-B102 (Vent worm, Lopez-Garcia *et al*., 2002)	97	–	–	–	–	–	–	+
	Gammaproteobacteria	Gammaproteobacterial clone SBseep6 (hydrocarbon seep, Santa Barbara, LaMontagne *et al*., 2004)	90–96	•	+	•	+	–	–	–
	Gammaproteobacteria	Bacterial clone ODP1230B1.23 (Peru margin site 1230, Inagaki *et al*., 2006)	90–98	•	•	+	•	+	•	+
	Deltaproteobacteria	Uncultured deltaproteobacterium DSS63 (Svalbard, Ravenschlag *et al*., 2000)	93	–	–	•	•	+	•	–

\+ Identification by sequencing.
• Identification by extrapolation of DGGE band position.
– Not present.
a. Shading shows depth ranges where sequences are consistently present.

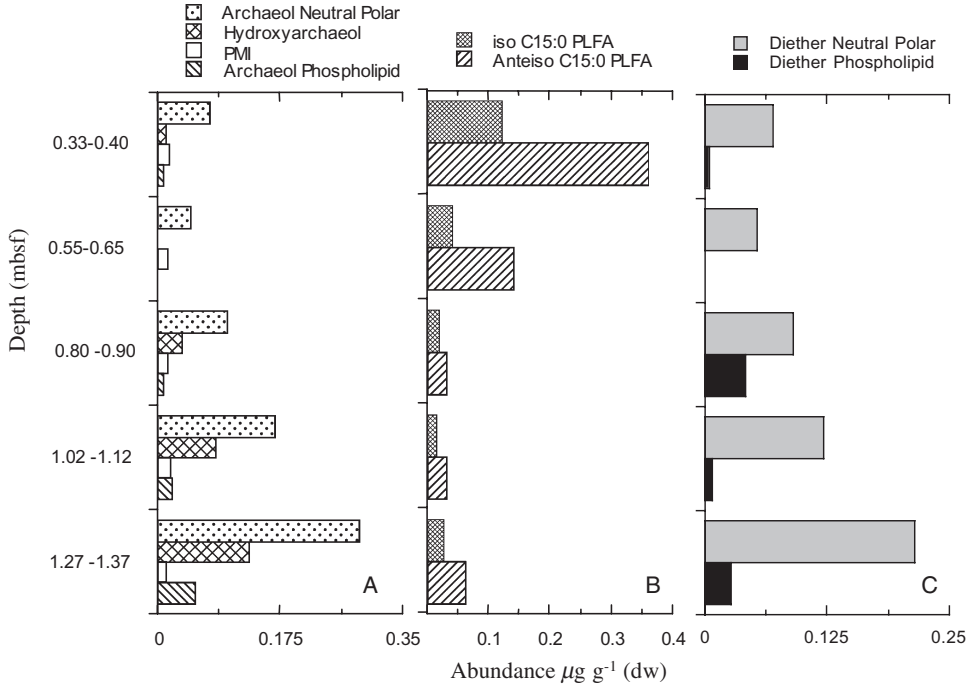

Fig. 5. Abundances of archaeal and bacterial lipid biomarkers in Skagerrak (Core 820) sediments. Shown are (A) abundances of archaeol (quantified both in the neutral lipid fraction and as a product of base hydrolysis of the phospholipid fraction), sn-2-hydroxyarchaeol and PMI; (B) C15 iso and anteiso-branched FFA; and (C) the abundances of non-isoprenoidal diethers comprising two C15 alkyl chains (albeit with different branching patterns) in both the neutral fraction and released by base hydrolysis of the phospholipid fraction.

as values found in cold seeps, nor the pore water methane at Site 821, it is still a low value relative to algal-derived organic matter (*c.* –20‰) and indicates that some carbon had been incorporated from ^{13}C-depleted CH_4. Potentially, this intermediate value suggests a source for archaeol from both methanogens and methanotrophs. Hydroxyarchaeol concentrations were lower (maximum concentration 0.13 μg g^{-1} compared with 0.29 μg g^{-1} for archaeol) but also increased with depth. Pentamethylicosane was also present in all samples but generally at much lower concentrations than other archaeal biomarkers (maximum concentration 0.03 μg g^{-1}) and with no clear depth trend. Bacterial biomarkers include iso and anteiso odd-chain branched fatty acids (including both C15:0 and C17:0), hopanoids and non-isoprenoidal diethers (Pancost *et al.*, 2001). The branched fatty acids were most abundant in the shallow sediments (0.3–0.4 m), and these have been previously interpreted as being derived from SRB (possibly *Desulfococcus* or *Desulfosarcina* species which can have high concentrations of these fatty acids, Rütters *et al.*, 2001; Elvert *et al.*, 2003; Blumenberg *et al.*, 2004; Webster *et al.*, 2006b) which are often associated with ANME groups (Knittel *et al.*, 2005; Orcutt *et al.*, 2005). Here, however, these compounds are likely to be predominantly from organisms involved with degradation of organic matter, due to their consistent decrease in abundances with depth and their relatively high $\delta^{13}C$ values (–25‰ to –28‰). Non-isoprenoidal diether lipids (three isomers, each comprised of two C15 alkyl units with either iso or anteiso methyl branching), which have been linked to AOM-associated SRB (e.g. Hinrichs *et al.*, 2000; Pancost *et al.*, 2001), had the opposite depth distributions, being present between 0.3 and 0.65 m but then increasing with depth to maximum values of 0.24 μg g^{-1} (summed abundance); crucially, their abundances closely parallel those of the archaeal biomarkers. In addition, phospholipid fraction diethers have higher concentrations in the deeper layers.

Overall, the lipid biomarker data demonstrate the presence of similar types of both *Archaea* and *Bacteria* in Skagerrak sediments to those indicated by the molecular genetic and activity data (Fig. 5). This suggests that the biomarker distributions are predominantly from active populations and reinforces the interpretation of the molecular genetic data.

Discussion

General overview

Skagerrak sediments have a clear sulfate reduction zone, a SMTZ, near which rates of AOM are maximal, and a deeper methanogenic zone; conditions which are

common for large areas of marine sediments controlled by diffusion. Many of the prokaryotes involved in AOM and methanogenesis at this site were similar to those present in the rather different seep and gas hydrate sediments, which have previously been the focus of AOM studies (Hinrichs *et al*., 1999; Boetius *et al*., 2000; Orphan *et al*., 2001; Orcutt *et al*., 2005). These include ANME-2a and ANME-3 sequences within the *Methanosarcinales* and *Deltaproteobacteria* which are AOM partners in other environments (Knittel *et al*., 2005). Lipid biomarkers for putative AOM prokaryotes were also present, including PMI, hydroxyarchaeol and archaeol for *Archaea*, and iso and anteiso C15:0 fatty acids and non-isoprenoidal diether lipids for SRB (Pancost *et al*., 2001; Blumenberg *et al*., 2004), supporting the molecular genetic evidence for the presence of prokaryotes involved in AOM and the direct measurement of active AOM (Fig. 1). These results are similar to those obtained for shallow water (~27 m), non-seep, Eckernforde Bay sediments in the German Baltic Sea, where ANME-2 were also the dominant AOM organisms (fluorescence *in situ* hybridization analysis) and the potential SRB syntrophic partner *Desulfosarcina–Desulfococcus* group were also present (Treude *et al*., 2005b). However, unlike the Skagerrak sediments, in Eckernforde Bay there was no sharp AOM peak at the SMTZ, possibly due to methane ebullition enhancing methane flux into a zone of sulfate wider than the SMTZ. It may be that the greater water depth of the Skagerrak sediments (308 m) sufficiently restricted methane ebullition to make it a truly diffusively controlled site, and hence, making this one of the first studies of the biogeochemistry and prokaryotic diversity of methane cycling in this type of location.

The majority of clones in the 1.39 m methanogen 16S rRNA gene library belonged to ANME groups within the *Methanosarcinales*. Sequences related to the H_2/CO_2 utilizing *Methanomicrobiales* group were the next most common followed by the acetate utilizing *Methanosaeta* group. Both the presence and relative abundance of these sequences fit with the comparative rate measurements of AOM, H_2/CO_2 and acetate methanogenesis at the same depth (Fig. 4). The predominance of CO_2 reduction with H_2 as a methanogenic pathway is also consistent with the highly negative $\delta^{13}C$ values of CH_4 *c.* –80‰ (Whiticar, 1999). Often individual ANME types dominate in different environments. For example, in a *Calyptogena* site above gas hydrates at Hydrate Ridge ANME-2c was dominant (Knittel *et al*., 2005) and ANME-2 sequences dominated the 'active' rRNA-derived sequences from an active mud volcano in the Gulf of Mexico (Martinez *et al*., 2006). However, in Black Sea microbial mats (Knittel *et al*., 2005) and North Sea gas seeps (Niemann *et al*., 2005), ANME-1 groups were dominant. The subsurface ANME community in the Skagerrak seems to be different from some other AOM communities by being dominated by the ANME-2a group. In addition, the Skagerrak differs from the seemingly similar, shallow, non-seep Eckernforde Bay sediments (Treude *et al*., 2005b) by the apparent absence of ANME-1 sequences. However, at 1.39 m the clone library is much deeper than most other studies and ANME sequences might have been different at shallower depths.

Methane flux

Depth integrated rates of AOM (1.73 mmol m^{-2} day^{-1}) are very similar to total rates of methanogenesis (1.70 mmol m^{-2} day^{-1}), and hence, AOM represents an effective barrier to methane release from these sediments, which is consistent with low methane concentrations above the zone of peak AOM rates (Fig. 1). However, clearly AOM and methanogenesis are finely balanced, and hence, potentially susceptible to environmental changes (e.g. increased organic matter input, temperature changes) which might lead to imbalance. This is in contrast to seep and gas hydrate systems where AOM has considerable capacity to oxidize increased methane flux (Kruger *et al*., 2005). Contiguous methane production and methane consumption in Skagerrak sediments is concentrated below the SMTZ at 0.7 m. This methane cycling is reflected in the deviation of $\delta^{13}C$-CH_4, between ~0.7 and 1.7 m (Fig. 1F), from the overall increasing trend in ^{13}C-content of CH_4. A situation which is consistent with ^{13}C-depleted CO_2 from methane oxidation being temporarily available for utilization by H_2/CO_2 methanogens (Borowski *et al*., 1997). There was also a broad stimulation in rates of H_2/CO_2 methanogenesis within the same zone (0.87–1.34 m), above the general trend for increasing rates with depth. Although, this is also suggestive of stimulated methane cycling, coupled with enhanced H_2 supply, it is difficult to know how meaningful this is, as there were other broad peaks in the H_2/CO_2 methanogenesis deeper in the profile. Acetate is also a potential intermediate in AOM (Valentine, 2002) and could also stimulate new CH_4 production. However, acetate is unlikely to be a substrate for methane recycling in the Skagerrak as acetate methanogenesis is close to zero during the peak in AOM and acetate concentrations decrease between ~0.6 and 1.4 m (Fig. 1). Interestingly, this zone also coincides with a decline in the rate of decrease in total cells and an increase in the numbers of dividing and divided cells (Fig. 2), which might indicate the presence of a zone of more active subsurface prokaryotic populations related to methane cycling (Parkes *et al*., 2005). The only ^{13}C-isotope value that could be obtained for archaeal biomarkers in these sediments was for archaeol which was $\delta^{13}C$ depleted (–55‰). This $\delta^{13}C$ value is further support for recycling of AOM-derived CO_2 which would provide the ^{13}C-depleted carbon for

incorporation into archaeal biomass, probably H_2/CO_2 methanogens. These results provide comprehensive documentation of the coupling of AOM and methanogenesis within a non-seep site. Similar coupling may occur at other locations as co-occurrence of AOM and methanogenesis is widespread in marine sediments (Kruger *et al*., 2005, Orcutt *et al*., 2005).

The depth distribution of assigned *Methanosaeta*-related, *Methanomicrobiales* and ANME T-RF peaks (42, 139 and 277) showed the same broad profile as their respective potential activities: acetate methanogenesis, H_2/CO_2 methanogenesis and AOM (Fig. 4B–D). This strongly suggests that these *Archaea* were responsible for driving the methane cycle in Skagerrak sediments. Although both methanogenesis and AOM are occurring in the same sediment layers, the depth distribution of these activities and their potential causative *Archaea* are not congruent (Fig. 4), which suggests that different organisms are catalysing the two processes. This unique data, directly quantifying the depth distribution of both AOM and methanogenic sequences, contrasts with recent results from some Gulf of Mexico seep sites suggesting that ANME organisms may be involved in both AOM and methanogenesis, but without directly measuring methanogen populations (Orcutt *et al*., 2005). This is despite the fact that the Skagerrak and Gulf of Mexico sediments have similar ratios of maximum rates of H_2/CO_2 methanogenesis and AOM (~1:5 and ~1:10 respectively), which was suggested to be a result of the same *Archaea* catalysing AOM and methanogenesis. However, the relationship between rates of AOM and methanogenesis may reflect methane recycling, as documented here, rather than both processes being catalysed by the same prokaryotes.

Archaea : Bacteria *interactions*

The presence of some general relationships between *Archaea* involved in methane flux and bacterial depth distributions (Fig. 4 and Table 1) in the Skagerrak suggests interaction between the two prokaryotic groups. For example, the sequences related (93%) to DSS63 SRB *Deltaproteobacteria* were present between 1.39 and 2.99 m where *Methanosaeta*-related T-RF peaks were abundant (Fig. 4D). In addition, the *Gammaproteobacteria* seep-related sequence (SBseep6) was present in the top 2 m, as was the uncultured *Chloroflexi*-related sequence, this distribution is similar to that of the ANME-2-related T-RF peak (Fig. 4C). The JS1 (OHKB2.83)- and OP8-related sequences were both present at 0.99 m and below, and although this does not correspond to any of the archaeal distributions it does support the suggestion that the candidate division JS1 is anaerobic and prefers low sulfate and high methane sedimentary environments (Webster *et al*., 2004). However, given the biases involved with PCR-based approaches and DGGE bacterial profiles being based on band presence or absence these need to be treated with caution.

Biomarker data also suggest the presence of SRB that may be associated with AOM, but in this case, two distinct types:

i. The high concentrations of iso and anteiso C15:0 between 0.3 and 0.65 m within the sulfate reduction and start of the AOM zones (Figs 1 and 5), have under similar circumstances, previously been considered as biomarkers for AOM-associated SRB within the *Desulfosarcina/Desulfococcus* group (Blumenberg *et al*., 2004). In addition, lower amounts of iso compared with anteiso C15:0 fatty acids, as found here, have also been interpreted as being indicative of SRB associated with ANME-1 *Archaea* at seep sites (Niemann *et al*., 2005). However, ANME-1 sequences were absent from our clone library and it may be that SRB : ANME associations in these diffusive controlled sediments are different from those at some seep sites. Conversely, in these sediments iso and anteiso C15:0 may be indicative of heterotrophic SRB as they decrease in concentration towards the peak AOM zone and have relatively high $\delta^{13}C$ values (–25‰ to –28‰).

ii. The other potential SRB biomarker, non-isoprenoidal diether lipids, also linked with AOM-associated SRB at other sites (Hinrichs *et al*., 2000; Pancost *et al*., 2001), had the opposite distribution, being at lowest concentration between 0.3 and 0.65 m and then increasing with depth (to 1.37 m, last depth analysed). This distribution fits with the deeper zone of less active AOM and perhaps indicates a change in the ANME-associated SRB partner at low AOM activity.

The DGGE sequence related to the *Desulfosarcina/Desulfococcus* group (93%, Table 1) had different depth distributions to both SRB biomarkers being only present below 0.99 m, and hence, might be involved in the deeper AOM activity, but could not be the source of these biomarkers.

The presence of 16S rRNA gene sequences and biomarkers both potentially related to SRB involved in AOM below the sulfate zone is rather surprising considering the requirement for sulfate. However, there is still some AOM activity below the SMTZ (Fig. 1), sulfate is still present at low concentrations (0.18 mM average concentration below 0.6 m) and other compounds might be used as alternative electron acceptors, such as iron oxides (Coleman *et al*., 1993) or humic acids (Lovley *et al*., 1996). In addition, AOM is not always coupled to sulfate reduction in other environments (e.g. Treude *et al*., 2005b; Orcutt *et al*., 2005). Interestingly, DGGE sequences related to both JS1 (OHKB2.83) and OP8

uncultured divisions had similar depth distributions to the non-isoprenoidal diether lipids (Table 1), which might indicate that these uncultured groups could be a source of these unusual bacterial lipids.

Conclusions

Overall, there is clear evidence for similar prokaryotes being involved in AOM at this diffusive site compared with AOM communities in many seep and gas hydrate sites, including AOM primarily being associated with sulfate reduction. This contrasts to the shallow marine, gassy sediments of Eckernforde Bay (German Baltic, Treude *et al*., 2005b) and Gulf of Mexico cold seeps (Orcutt *et al*., 2005) where AOM appears to be uncoupled from sulfate reduction. In addition, although there is overlap between AOM and methanogenesis in Skagerrak sediments, the location of their maximum activities and distribution of causative prokaryotes are distinct, demonstrating that different microorganisms are catalysing AOM and methanogenesis, despite the suggestion that in some seep environments the same prokaryotes are responsible for both activities. Methane production and AOM is surprisingly tightly coupled in these diffusive sediments, which suggests that methane flux from these sediments might be sensitive to environmental change.

Experimental procedures

Site description and sampling

Sediment to 4.9 and 4.25 m depth was sampled with two gravity cores (GC) in the Skagerrak, off the Danish coast, on the METROL Heincke 191 cruise, sites 820/821GC (58°2.246′N, 9°37.963′E) from ~308 m water depth. Site 821 sediment was used for all analyses except that for lipid biomarkers (due to the large sample volume required), which predominantly came from a separate core (Site 820) at the same location and with the same geochemical profile as core 821. Immediately after retrieval, the cores were cut into 1-m-long sections. Before the sectioned core liner was capped: (i) sediment was sampled from the top of the sediment for *in situ* CH_4 concentrations; (ii) temperature was measured; (iii) pH was measured. The capped sections were stored upright, cooled, until CH_4 concentration data were obtained. Based on these data sampling intervals were selected to ensure effective sampling around the SMTZ. One-metre core sections were placed horizontally in a cutting rig and two 20 cm long × 2 cm diameter Plexiglas mini-cores were pressed 10 cm into the sediment for measurement of acetate metabolism and H_2/CO_2 methanogenesis. Samples for AOM were taken as triplicates in 1 cm diameter glass tubes at 5 cm intervals. The sediment core was extruded from the GC-core liner, using a piston, until the bottom of the inserted mini-cores were in line with the rim of the GC core liner and the extruded mud cut off. The subcores were closed with rubber stoppers, gently washed and stored at *in situ* temperature until further treatment. In addition, during the above sampling two 3 cm diameter mini-cores were taken for porosity and for pore-water (from squeezers, for volatile fatty acids, dissolved inorganic carbon and sulfate). Two 50 ml sterile syringes, with top end removed, were used to obtain samples (40 cm^3) for molecular genetics. Two 5 ml cut-off syringes were used to obtain samples (1 cm^3) for acridine orange direct count [AODC, stored in glass vials with 9 ml of 2% filter sterilized (0.2 μm) formaldehyde in 3.5% NaCl] and a detailed methane profile (3 cm^3). From the parallel core (820) sediment samples (~300 cm^3) for lipid analysis were aseptically cut from the extruded core using a sterile cheese wire, then wrapped in furnaced aluminium foil and frozen at −20°C. Loss of surface sediment during gravity coring was calculated by comparison of sulfate profiles with non-disturbed samples collected with a Rumohr Lot or Multi corer, and the gravity core depth adjusted accordingly. The two gravity cores were similarly aligned using the sulfate profile.

Biogeochemistry

Depth distributions of prokaryotic activity was measured with radiotracers under conditions as close as possible to those *in situ*; however, as these were conducted on recovered sediments results need to be considered as potential measurements. This still enables effective comparison of rates at different depths and between different activities. Methane concentrations were determined from sediment samples sealed in glass tubes containing 6 ml NaOH (2.5% w/v). The headspace was analysed by gas chromatography (GC, 5890A, Hewlet Packard) with a packed stainless steel Porapak-Q column (6 ft, 0.125 in., 80/100 mesh, Agilent Technology) and a flame ionization detector. Helium was the carrier gas, and column temperature was 40°C. Dissolved inorganic carbon concentrations were determined from 1.25 ml samples of pore water, fixed with 20 μl $HgCl_2$ and sealed, without headspace, in a glass vial using the rapid small volume flow injection method of measuring aqueous CO_2 (Hall and Aller, 1992). Pore water sulfate and acetate concentrations were measured by ion exchange chromatography using an ICS-2000 ion chromatography system (Dionex®, UK) fitted with two AS15-HC 4 mm columns in series, and a Dionex® Anion Self-Regenerating Suppressor (ASRS®-ULTRA II 4-mm) unit in combination with a Dionex® DS6 heated conductivity cell. Components were separated using a potassium hydroxide gradient program as follows: 6.0 mM KOH (38 min isocratic), 16.0 mM KOH min^{-1} to 70 mM (17 min isocratic).

Rates of methanogenesis were measured using ^{14}C-labelled acetate or bicarbonate radiotracers. Samples that had been stored at *in situ* temperature (16°C) overnight were injected with either undiluted ^{14}C-labelled sodium [2-^{14}C] acetate (2 μl, 20 kBq) or sodium [^{14}C] bicarbonate (2 μl of a 1:4 dilution, 38.5 kBq) and then incubated at 16°C for 7 h (acetate) or 17–21 h (bicarbonate). Injections every 2 cm were made through silicone-covered ports in the side of the mini-cores. Between one and four injections were made into each mini-core depending on the resolution required. Incubations were terminated by extruding the sediment sample into glass jars containing 7 ml of 5 M NaOH. Jars were sealed tightly with butyl rubber bungs, shaken and stored upside down before processing. $^{14}CH_4$ was stripped from the jar by

flushing with a 95:5 nitrogen : oxygen mix (70 ml min^{-1} for 25 min), oxidized to $^{14}CO_2$ in a CuO furnace operated at 800°C (Cragg *et al*., 1992) and trapped in β-phenethylamine [0.7% v/v in OptiPhase 'HiSafe' 3 (Perkin Elmer) scintillation cocktail] for counting by a TriCarb 2900TR liquid scintillation counter (Packard). Acetate oxidation rates were subsequently determined from the same samples as those for acetate methanogenesis. A subsample of the slurry was acidified with 5 M HCl and evolved $^{14}CO_2$ trapped with β-phenethylamine (0.7%v/v in OptiPhase 'HiSafe' 3 scintillation cocktail, Perkin Elmer). Methane production and acetate oxidation rates were calculated based on the proportion of labelled gas produced from the ^{14}C-substrate, and the dissolved pore water acetate or total CO_2 concentrations adjusted for sediment porosity and incubation time. Samples for AOM measurement were injected with ^{14}C-CH_4 (15 μl, 1.5 kBq) and incubated for 12 h at *in situ* temperature. The incubation was stopped in NaOH (2.5% w/v) as above. The total methane pool of the sample was determined by GC analysis of the headspace, the fraction of labelled methane was measured by combustion to ^{14}C-CO_2, and the amount of produced ^{14}C-CO_2 was analysed by acidification with 5 ml HCl (6 M) and trapping of the total CO_2 in phenethylamine. Rates of anaerobic oxidation of methane were calculated according to Treude and colleagues (2003). Total prokaryote numbers were determined by AODC counts as previously described (Parkes *et al*., 2005). Trends and peaks in rate and AODC data were assessed by analysis of variance, the sum of squares simultaneous test procedure and the Mood-median test, as appropriate by Mini-Tab 14.2.

Gases were stripped from pore water for $\delta^{13}C$ analysis according to the method of McAullife (1971). The gas was stored as a headspace in inverted crimp top Wheaton® vials by displacement of a preservative solution that consisted of 10 wt% KCl in deionized water adjusted to pH 1 using HCl. Stable carbon isotope analysis of CH_4 was conducted by GC combustion isotope ratio mass spectrometry using a Varian 3400® GC coupled to a Thermoelectron XP® mass spectrometer via a Gas Bench® interface. Methane was separated on a PLOT Q capillary column (0.32 mm × 30 m) and combusted to CO_2 at 1000°C in a ceramic reactor containing Cu and Pt wires. A high purity blend of 1% O_2 in helium was fed into the reactor at ~0.1 ml min^{-1} to ensure quantitative conversion of CH_4 to CO_2. The H_2O produced was removed using a Nafion® membrane. Accuracy and precision of $\delta^{13}C$-CH_4 analysis by this method were both better than ± 0.2‰ based upon replicate analysis of a BOC alpha gravimetric CH4 standard. Stable isotope ratios are reported in the standard delta (™^{13}) notation in units of per mil (‰) relative to Vienna Pee Dee Belemnite.

DNA extraction

DNA was extracted and purified from the 0.25, 0.99, 1.39, 1.86, 2.43, 2.99 and 3.80 m depth subsamples (0.5 g in duplicate) using the FastDNA Spin Kit for Soil (Q-BIOgene) with the modifications detailed by Webster and colleagues (2003). Duplicate extractions were pooled, concentrated and purified by dialysis with sterile water in Microcon YM-100 centrifugal filters (Millipore Corporation) to give a final volume of 100 μl.

PCR amplification construction and analysis of methanogen 16S rRNA gene library

DNA extracted from the 1.39 m depth subsample was used for the construction of a methanogen 16S rRNA gene library. DNA was amplified by PCR using primers 355F (3′-CAGG CGCGAAAACTTTAC-5′) and 1068R (3′-ATGCTTCACAGTA CGAAC-5′); previously developed to specifically target members of *Methanosarcinales* and *Methanomicrobiales* (Banning *et al*., 2005). Polymerase chain reactions were performed using a Dyad DNA Engine (MJ Research) thermal cycler with an initial denaturation step of 94°C for 5 min followed by 30 cycles of 94°C for 1 min, 52°C for 1 min and 72°C for 1 min 30 s and a final elongation step of 72°C for 5 min. Five replicate PCR amplifications were pooled, purified, cloned, sequenced and sequences analysed as described previously (Banning *et al*., 2005). Sequences generated in this study have been deposited in the GenBank database under accession numbers DQ988142 to DQ988151.

Methanogen 16S rRNA gene T-RFLP analysis

Polymerase chain reaction amplification of DNA from all depths, described above, was performed using the same methanogen-specific primers as for the 16S rRNA gene library construction but with a 5′ label of 6-carboxyfluorescein (FAM) attached to the forward primer. The method described previously by Banning and colleagues (2005) was modified to include a dual enzyme digest with TaqI and RsaI to reduce the T-RFs of all *Methanosarcinales* to 280 bp. The predicted T-RFs of *Methanosaeta* spp. and members of *Methanomicrobiales* remained unchanged. The predicted size of the T-RFs from this study are shown in Table 2. Some T-RFs detected in the T-RFLP profiles could not be identified by *in silico* analysis of cultured methanogen and methanogen clone sequences available through the RDP. The T-RF sizes of sequences recovered in the 16S rRNA gene library presented in this study were also predicted by *in silico* analysis and did not match any of the unknown T-RFs. These unaffiliated T-RFs accounted for a mean of 2.6% of all peaks.

Dual restriction digests of the PCR amplicons were performed by incubating 100 ng of the PCR amplicons with 5 U of TaqI (Promega) at 65°C for 2 h followed by incubation at 37°C for 2 h with 5 U of added RsaI (Promega). Reactions were carried out in Buffer C containing 2 μg of BSA in 20 μl total volumes. Restriction products were diluted to 500 μl with sterile water and passed through Microcon YM-10 centrifugal filters (Millipore, MA, USA). Desalted restriction products were analysed on an ABI 3100 Prism Genetic Analyzer automated capillary sequencer and peak heights quantified using GeneScan Analysis v3.7 software (Applied Biosystems) as described previously (Banning *et al*., 2005). Signals with a peak height below 100 relative fluorescent units (rfu) and signals with a peak height below 250 rfu that occurred only once in all depth profiles were excluded from the analysis.

PCR-DGGE analysis of bacterial 16S rRNA genes

Bacterial and candidate division JS1 16S rRNA genes were amplified from sediment DNA extracts using the general bacterial primers 27F (5-AGAGTTTGATCMTGGCTCAG-3′) and

Table 2. Potential methanogen species or 16S rRNA gene sequences responsible for T-RFs recovered from Skagerrak.

T-RF measured[a] (predicted[b])	Example methanogens with appropriate T-RF	Potential substrate utilization
42 (46)	*Methanosaeta concilii*[c] *Methanoculleus bourgense* (and other spp.) Sk6C-20, Sk6C-21	Acetate only H_2/CO_2, formate, secondary alcohols
– (129)	SYA-45 (AF126846)	Unknown
139 (144)	*Methanospirillum hungatei*[c] *Methanoplanus limicola* *Methanogenium organophilum* (and other spp.) *Methanogenium cariaci* *Methanofollis tationis* (and *limitans*) Sk6C-14, Sk6C-31, Sk6C-1, Sk6C-18	H_2/CO_2, formate, secondary alcohols
– (148)	S30-2 (Rice Cluster I; AJ236514) S30-29 (Rice Cluster II; AJ236538)	Unknown
277 (280)	*Methanosarcina barkeri*[c] (and other spp.) *Methanolobus taylorii* (and other spp.) *Methanohalophilus mahii* *Methanococcoides butonii* (and other spp.) *Methanomethylovorans hollandica*	All can use methyl compounds. Some use acetate. Some use H_2/CO_2 but never formate.
– (280)	ANME groups 1a, 1b, 2a and 3 sequences (e.g. AF354130, AF354134, AJ579327, AJ578119, AB019758, AB019759, AJ578130, AF354137, AJ578129, AJ578084) Sk6C-23, Sk6C-30, Sk6C-32, Sk6C-44	Anaerobic oxidation of methane
– (57)	ANME-2b sequences (e.g. AF354140, AF354128, AF354138)	Anaerobic oxidation of methane
– (195)	ANME-2c sequences (e.g. AF354131, AF419638, AF354133)	Anaerobic oxidation of methane

a. Measured T-RFs varied by up to 2 bp between replicate runs; – indicates T-RF could not be verified against cultivated strains since only matches to uncultivated phylotypes.
b. Predicted by *in silico* analysis.
c. Measured T-RF confirmed by analysis of DNA from pure cultures of type strains of indicated species.

907R (5′-CCGTCAATTCMTTTGAGTTT-3′), and the JS1-targeted primers 63F (5′-CAGGCCTAACACATGCAAGTC-3′) and 665R (5′-ACCGGGAATTCCACYTYCCT-3′) as previously described (Webster *et al*., 2004; 2006b). The JS1 candidate division has previously been shown to be present in low sulfate sediments with methane, and hence, might dominate zones of the Skagerrak sediment as it does in other environments (Webster *et al*., 2004) All bacterial 16S rRNA gene PCR products (including JS1) were then re-amplified by nested PCR with primers 357F (5′-CCTACGGGAGG CAGCAG-3′) with a GC clamp at the 5′ end (Muyzer *et al*., 1993) and 518R (5′-ATTACCGCGGCTGCTGG-3′) as described (Webster *et al*., 2003). Polymerase chain reaction amplimers were analysed by DGGE (Webster *et al*., 2003) using the DCode system (Bio-Rad) on 8% (w/v) polyacrylamide gels with a denaturant gradient between 30% and 60% [100% denaturant equals 7 M urea and 40% (v/v) formamide]. Gels were stained with SYBRGold nucleic acid stain (Molecular Probes), viewed under UV and images captured using a Gene Genius Bio Imaging System (Syngene). DGGE bands of interest were excised, re-amplified by PCR (Webster *et al*., 2006b), sequenced using an ABI PRISM 3100-Genetic Analyzer and sequences deposited under accession numbers AM421906 to AM421934.

Bacterial sequence and phylogenetic analysis

Sequence chromatographs were analysed using the Chromas software package version 1.45 (http://www.technelysium.com/au/chromas.html). Partial bacterial 16S rRNA gene sequences were subjected to a nucleotide-nucleotide BLAST (BLASTN) search at NCBI to identify sequences from current nucleotide database with highest sequence similarity. Details of these and phylogenetic analysis methods were described previously (Webster *et al*., 2004; Banning *et al*., 2005).

Lipid extraction, fractionation, derivatization and gas chromatographic determination

Samples of the frozen sediment (~25 g) were freeze-dried and extracted for 24 h with Soxhlet apparatus and a DCM : MeOH mixture (2:1 v/v). Elemental sulfur was removed from the total lipid extracts (TLE) by adding ~100 mg of activated copper and stirring for 4 h. Aliquots of the TLE were separated into three operationally defined fractions using pre-washed 500 mg amino-propyl (55 μm, 70 Å) columns (Phenomenex, USA). A series of isopropanol/DCM (2:1 v/v), 2% acetic acid in diethyl ether and methanol were used to elute the neutral, free fatty acid (FFA) and phospholipid fatty acid (PLFA) fractions respectively. The neutral fraction was further separated into apolar and polar fractions using an alumina column and three times the column volume of hexane/DCM (9:1 v/v) and DCM/MeOH (1:2 v/v) to elute the two fractions respectively. Fatty acids in the FFA and PLFA fractions were methylated into fatty acid methyl esters by refluxing at 70°C for 1 h with BF3 (14% in MeOH). Alcohols in the neutral polar, FFA and PLFA fractions were con-

verted to their trimethylsilyl derivatives using 25 μl of each N,O-bis(trimethylsilyl)trifluoroacetamide and pyridine heated at 70°C for 1 h.

All fractions were screened initially by GC using a Carlo-Erba HRGC 5400 mega series with a flame ionization detector and a Chrompack fused silica capillary column (50 m length, 0.32 mm internal diameter) with a non-polar CP-Sil 5 CB stationary phase (dimethylpolysiloxane equivalent, film thickness 0.12 μm). Compounds were identified on a Thermoquest Finnigan Trace GC interfaced to a Thermoquest Finnigan Trace MS operating with electron ionization at 70 eV and scanning an m/z range of 50–850. Gas chromatography conditions for GC-MS analyses are the same as for GC analyses as described above.

Acknowledgements

This research was funded by the EU METROL Project plus grants from the UK NERC M and FMB programme. We thank the Captain, crew and scientists on Heincke 191 Cruise for their assistance and I.D. Bull and R. Berstan of the NERC Life Sciences Mass Spectrometry Facility for analytical support for the biomarker analysis. We acknowledge the informative and stimulating interaction we had with other members of the METROL Project and referees for their constructive comments and suggestions.

References

Banning, N., Brock, F., Fry, J.C., Parkes, R.J., Hornibrook, E.R.C., and Weightman, A.J. (2005) Investigation of the methanogen population structure and activity in a brackish lake sediment. *Environ Microbiol* **7:** 947–960.

Bian, L.Q., Hinrichs, K.U., Xie, T.M., Brassell, S.C., Iversen, H., Fossing, H., *et al.* (2001) Algal and archaeal polyisoprenoids in a recent marine sediment: molecular isotopic evidence for anaerobic oxidation of methane. *Geochem Geophys Geosystems* **2:** art no. 2000GC000112.

Blumenberg, M., Seifert, R., Reitner, J., Pape, T., and Michaelis, W. (2004) Membrane lipid patterns typify distinct anaerobic methanotrophic consortia. *Proc Natl Acad Sci USA* **101:** 11111–11116.

Boetius, A., Ravenschlag, K., Schubert, C.J., Rickert, D., Widdel, F., Gieseke, A., *et al.* (2000) A marine microbial consortium apparently mediating anaerobic oxidation of methane. *Nature* **407:** 623–626.

Borowski, W.S., Paull, C.K., and Ussler, W. (1997) Carbon cycling within the upper methanogenic zone of continental rise sediments: an example from the methane-rich sediments overlying the Blake Ridge gas hydrate deposits. *Mar Chem* **57:** 299–311.

Bouloubassi, I., Aloisi, G., Pancost, R.D., Hopmans, E., Pierre, C., and Sinninghe Damste, J.S. (2006) Archaeal and bacterial lipids in authigenic carbonate crusts from eastern Mediterranean mud volcanoes. *Org Geochem* **37:** 484–500.

Coleman, M.L., Hedrick, D.B., Lovley, D.R., White, D.C., and Pye, K. (1993) Reduction of Fe(Iii) in sediments by sulfate-reducing bacteria. *Nature* **361:** 436–438.

Cragg, B.A., Harvey, S.M., Fry, J.C., Herbert, R.A., and Parkes, R.J. (1992) Bacterial biomass and activity in the deep sediment layers of the Japan Sea, Hole 798B. *Proc ODP Sci Res* **127/128:** 761–776.

Dong, H., Zhang, G., Jiang, H., Yu, B., Chapman, L., Lucas, C., and Fields, M. (2006) Microbial diversity in sediments of Saline Qinghai Lake, China: linking geochemical controls to microbial ecology. *Microb Ecol* **51:** 65–82.

van Dongen, B.E., Irene, C., Rijpstra, W., Philippart, C.J.M., de Leeuw, J.W., and Sinninghe Damste, J.S. (2000) Biomarkers in upper Holocene Eastern North Sea and Wadden Sea sediments. *Organic Geochem* **31:** 1533.

Eglinton, G., and Hamilton, R.J. (1967) Leaf epicuticular waxes. *Science* **156:** 1322–1335.

Elvert, M., Boetius, A., Knittel, K., and Jørgensen, B.B. (2003) Characterization of specific membrane fatty acids as chemotaxonomic markers for sulfate-reducing bacteria involved in anaerobic oxidation of methane. *Geomicrobiol J* **20:** 403–419.

Fang, J., Shizuka, A., Kato, C., and Schouten, S. (2006) Microbial diversity of cold-seep sediments in Sagami Bay, Japan, as determined by 16S rRNA gene and lipid analyses. *FEMS Microbiol Ecol* **227:** 48–66.

Hall, P.O.J., and Aller, R.C. (1992) Rapid small volume flow injection analysis for CO2 and NH4+ in marine and freshwaters. *Limnol Oceanogr* **37:** 1113–1118.

Hinrichs, K.U., Hayes, J.M., Sylva, S.P., Brewer, P.G., and DeLong, E.F. (1999) Methane-consuming archaebacteria in marine sediments. *Nature* **398:** 802–805.

Hinrichs, K.U., Summons, R.E., Orphan, V., Sylva, S.P., and Hayes, J.M. (2000) Molecular and isotopic analysis of anaerobic methane-oxidizing communities in marine sediments. *Org Geochem* **31:** 1685–1701.

Inagaki, F., Suzuki, M., Takai, K., Oida, H., Sakamoto, T., Aoki, K., *et al.* (2003) Microbial communities associated with geological horizons in coastal subseafloor sediments from the Sea of Okhotsk. *Appl Environ Microbiol* **69:** 7224–7235.

Inagaki, F., Nunoura, T., Nakagawa, S., Teske, A., Lever, M., Lauer, A., *et al.* (2006) Biogeographical distribution and diversity of microbes in methane hydrate-bearing deep marine sediments, on the Pacific Ocean Margin. *Proc Natl Acad Sci USA* **103:** 2815–2820.

Iversen, N., and Jørgensen, B.B. (1985) Anaerobic methane oxidation rates at the sulfate-methane transition in marine sediments from Kattegat and Skagerrak (Denmark). *Limnol Oceanogr* **30:** 944–955.

Knittel, K., Losekann, T., Boetius, A., Kort, R., and Amann, R. (2005) Diversity and distribution of methanotrophic archaea at cold seeps. *Appl Environ Microbiol* **71:** 467–479.

Kruger, M., Treude, T., Wolters, H., Nauhaus, K., and Boetius, A. (2005) Microbial methane turnover in different marine habitats. *Palaeogeogr Palaeoclimatol Palaeoecol* **227:** 6–17.

Kvenvolden, K.A. (1988) Methane hydrate – a major reservoir of carbon in the shallow geosphere. *Chem Geol* **71:** 41–51.

LaMontagne, M.G., Leifer, I., Bergmann, S., Van De Werf-horst, L.C., and Holden, P.A. (2004) Bacterial diversity in

marine hydrocarbon seep sediments. *Environ Microbiol* **6:** 799–808.

Lopez-Garcia, P., Gaill, F., and Moreira, D. (2002) Wide bacterial diversity associated with tubes of the vent worm Riftia pachyptila. *Environ Microbiol* **4:** 204–215.

Lovley, D.R., and Chapelle, F.H. (1995) Deep subsurface microbial processes. *Rev Geophys* **33:** 365–381.

Lovley, D.R., Coated, J.D., Blunt-Harris, E.L., Phillips, E.L., and Woodward, J.C. (1996) Humic substances as electron acceptors for microbial respiration. *Nature* **382:** 445–448.

McAullife, C. (1971) GC determination of solutes by multiple phase equilibration. *Chem Technol* **1:** 46–51.

Marlowe, I.T., Green, J.C., Neal, A.C., Brassell, S.C., Eglinton, G., and Course, P.A. (1984) Long-Chain (N-C37-C39) alkenones in the prymnesiophyceae – distribution of alkenones and other lipids and their taxonomic significance. *Br Phycol J* **19:** 203–216.

Martinez, R.J., Mills, H.J., Story, S., and Sobecky, P.A. (2006) Prokaryotic diversity and metabolically active microbial populations in sediments from an active mud volcano in the Gulf of Mexico. *Environ Microbiol* **8:** 1783–1796.

Muyzer, G., Dewaal, E.C., and Uitterlinden, A.G. (1993) Profiling of complex microbial-populations by denaturing gradient gel-electrophoresis analysis of polymerase chain reaction-amplified genes-coding for 16s ribosomal-RNA. *Appl Environ Microbiol* **59:** 695–700.

Newberry, C.J., Webster, G., Cragg, B.A., Parkes, R.J., Weightman, A.J., and Fry, J.C. (2004) Diversity of prokaryotes and methanogenesis in deep subsurface sediments from the Nankai Trough, Ocean Drilling Program Leg 190. *Environ Microbiol* **6:** 274–287.

Niemann, H., Elvert, M., Hovland, M., Orcutt, B., Judd, A., Suck, I., *et al.* (2005) Methane emission and consumption at a North Sea gas seep (Tommeliten area). *Biogeosciences* **2:** 335–351.

Orcutt, B., Boetius, A., Elvert, M., Samarkin, V., and Joye, S.B. (2005) Molecular biogeochemistry of sulfate reduction, methanogenesis and the anaerobic oxidation of methane at Gulf of Mexico cold seeps. *Geochim Cosmochim Acta* **69:** 4267–4281.

Orphan, V.J., House, C.H., Hinrichs, K.U., McKeegan, K.D., and DeLong, E.F. (2001) Methane-consuming archaea revealed by directly coupled isotopic and phylogenetic analysis. *Science* **293:** 484–487.

Pancost, R.D., and Damste, J.S.S. (2003) Carbon isotopic compositions of prokaryotic lipids as tracers of carbon cycling in diverse settings. *Chem Geol* **195:** 29–58.

Pancost, R.D., Hopmans, E.C., and Damste, J.S.S. (2001) Archaeal lipids in Mediterranean cold seeps: molecular proxies for anaerobic methane oxidation. *Geochim Cosmochim Acta* **65:** 1611–1627.

Pancost, R.D., Zhang, C.L., Tavacoli, J., Talbot, H.M., Farrimond, P., Schouten, S., *et al.* (2005) Lipid biomarkers preserved in hydrate-associated authigenic carbonate rocks of the Gulf of Mexico. *Palaeogeogr Palaeoclimatol Palaeoecol* **227:** 48–66.

Parkes, R.J., Webster, G., Cragg, B.A., Weightman, A.J., Newberry, C.J., Ferdelman, T.G., *et al.* (2005) Deep subseafloor prokaryotes stimulated at interfaces over geological time. *Nature* **436:** 390–394.

Peterson, S.B., Dunn, A.K., Klimowicz, A.K., and Handelsman, J. (2006) Peptidoglycan from *Bacillus cereus* mediates commensalism with rhizosphere bacteria from the *Cytophaga-Flavobacterium* group. *Appl Environ Microbiol* **72:** 5421–5427.

Ravenschlag, K., Sahm, K., Knoblauch, C., Jørgensen, B.B., and Amann, R. (2000) Community structure, cellular rRNA content, and activity of sulfate-reducing bacteria in marine Arctic sediments. *Appl Environ Microbiol* **66:** 3592–3602.

Reed, D.W., Fujita, Y., Delwiche, M.E., Blackwelder, D.B., Sheridan, P.P., Uchida, T., and Colwell, F.S. (2002) Microbial communities from methane hydrate-bearing deep marine sediments in a forearc basin. *Appl Environ Microbiol* **68:** 3759–3770.

Rütters, H., Sass, H., Cypionka, H., and Rullkotter, J. (2001) Monoalkylether phospholipids in the sulfate-reducing bacteria *Desulfosarcina variabilis* and *Desulforhabdus amnigenus*. *Arch Microbiol* **176:** 435–442.

Süß, J., Engelen, B., Cypionka, H., and Sass, H. (2004) Quantitative analysis of bacterial communities from Mediterranean sapropels based on cultivation-dependent methods. *FEMS Microbiol Ecol* **51:** 109–121.

Teske, A., Hinrichs, K.U., Edgcomb, V., Gomez, A.D., Kysela, D., Sylva, S.P., *et al.* (2002) Microbial diversity of hydrothermal sediments in the Guaymas Basin: evidence for anaerobic methanotrophic communities. *Appl Environ Microbiol* **68:** 1994–2007.

Treude, T., Boetius, A., Knittel, K., Wallmann, K., and Jorgensen, B.B. (2003) Anaerobic oxidation of methane above gas hydrates at Hydrate Ridge, NE Pacific Ocean. *Mar Ecol Prog Ser* **264:** 1–14.

Treude, T., Knittel, K., Blumenberg, M., Seifert, R., and Boetius, A. (2005a) Subsurface microbial methanotrophic mats in the Black Sea. *Appl Environ Microbiol* **71:** 6375–6378.

Treude, T., Kruger, M., Boetius, A., and Jørgensen, B.B. (2005b) Environmental control on anaerobic oxidation of methane in the gassy sediments of Eckernforde Bay (German Baltic). *Limnol Oceanogr* **50:** 1771–1786.

Valentine, D.L. (2002) Biogeochemistry and microbial ecology of methane oxidation in anoxic environments: a review. *Antonie Van Leeuwenhoek Int J Gen Mol Microbiol* **81:** 271–282.

Webster, G., Newberry, C.J., Fry, J.C., and Weightman, A.J. (2003) Assessment of bacterial community structure in the deep sub- seafloor biosphere by 16S rDNA-based techniques: a cautionary tale. *J Microbiol Methods* **55:** 155–164.

Webster, G., Parkes, R.J., Fry, J.C., and Weightman, A.J. (2004) Widespread occurrence of a novel division of bacteria identified by 16S rRNA gene sequences originally found in deep marine sediments. *Appl Environ Microbiol* **70:** 5708–5713.

Webster, G., Parkes, R.J., Cragg, B.A., Newberry, C.J., Weightman, A.J., and Fry, J.C. (2006a) Prokaryotic community composition and biogeochemical processes in deep subseafloor sediments from the Peru Margin. *FEMS Microbiol Ecol* **58:** 65–85.

Webster, G., Watt, L., Rinna, J., Fry, J.C., Evershed, R.P., Parkes, R.J., and Weightman, A. (2006b) A comparison of stable-isotope probing of DNA and phospholipid fatty acids to study prokaryotic functional diversity in sulfate-reducing marine sediment enrichment slurries. *Environ Microbiol* **8:** 1575–1589.

Whiticar, M.J. (1999) Carbon and hydrogen isotope systematics of bacterial formation and oxidation of methane. *Chem Geol* **161:** 291–314.

Zhang, C.L., Pancost, R.D., Sassen, R., Qian, Y., and Macko, S.A. (2003) Archaeal lipid biomarkers and isotopic evidence of anaerobic methane oxidation associated with gas hydrates in the Gulf of Mexico. *Org Geochem* **34:** 827–836.

